

Spin-Orbital Entangled Excitonic Insulators in $(t_{2g})^4$ Correlated Electron Systems

Toshihiro Sato¹, Tomonori Shirakawa², and Seiji Yunoki^{1,2,3}

¹*Computational Condensed Matter Physics Laboratory, RIKEN, Wako, Saitama 351-0198, Japan*

²*Computational Quantum Matter Research Team,*

RIKEN Center for Emergent Matter Science (CEMS), Wako, Saitama 351-0198, Japan

³*Computational Materials Science Research Team,*

RIKEN Advanced Institute for Computational Science (AICS), Kobe, Hyogo 650-0047, Japan

(Dated: September 11, 2018)

We employ the multi-orbital dynamical mean-field theory to examine the ground state of a three-orbital Hubbard model with a relativistic spin-orbit coupling (SOC) at four electrons per site. We demonstrate that the interplay between the strong electron correlations and the SOC induces a Van Vleck-type nonmagnetic insulator and its magnetic exciton condensation. We also find in the moderate electron correlation regime that the SOC induces another type of a nonmagnetic excitonic insulator, in addition to a relativistic band insulator. The characteristic features among these insulators are manifested in the momentum resolved single-particle excitations, thus accessible by angle-resolved photoemission spectroscopy experiments.

PACS numbers: 71.27.+a, 71.30.+h, 75.25.Dk

Since the observation of an antiferromagnetic (AF) insulator in 5d transition metal Ir oxides $A_2\text{IrO}_4$ ($A = \text{Sr}$ and Ba) [1–5], many properties of the insulator have been explored both theoretically and experimentally. These materials are crystalized in a layered perovskite structure with nominally five 5d electrons per Ir in t_{2g} orbitals which are separated from e_g orbitals due to a large crystal field. The important difference from 3d and 4d transition metal oxides is that 5d transition metal oxides show a strong relativistic spin-orbit coupling (SOC) along with the moderate electron correlations. Because of the strong SOC, t_{2g} orbitals are split into the local effective total angular momentum $j = 1/2$ doublet and $j = 3/2$ quartet in the atomic limit [6]. The theoretical and experimental studies have revealed the AF insulating ground state with the half-filled $j = 1/2$ based band, where the $j = 3/2$ based bands are completely occupied [7–18]. The low temperature phase diagram in the $(t_{2g})^5$ electron system has also been reported theoretically, focusing on the competition between the electron correlations and the SOC [19]. It has been also predicted that the carrier doping can induce unconventional superconductivities [20–23].

Recently, two experiments have reported interesting observations for perovskite and post-perovskite 5d transition metal oxides, AOsO_3 ($A = \text{Ca}, \text{Sr}, \text{and Ba}$) [24, 25] and NaIrO_3 [26], respectively, with a nominally $(t_{2g})^4$ electron configuration. At low temperatures, all these materials except for SrOsO_3 exhibit an insulating behavior with no indication of magnetic order, despite that the first-principles calculations based on density functional theory (DFT), including LDA(GGA)+SOC+ U calculations, predict that these materials are all metallic [24, 26–28].

When the SOC is significantly large, i.e., in the jj coupling limit, the $j = 1/2$ and $3/2$ based bands are well separated to simply become a relativistic band insulator

with the fully occupied $j = 3/2$ based bands and the completely empty $j = 1/2$ based band. Indeed, Du *et al.* has performed the LDA+Gutzwiller calculation, which combines the DFT with the local density approximation (LDA) and the Gutzwiller variational method, and concluded that NaIrO_3 is such a correlated paramagnetic band insulator [27, 29].

On the other hand, when the electron correlations are dominant, the LS coupling scheme in the atomic limit is a better description. According to the Hund's rule, the ground state of a $(t_{2g})^4$ electron system has the orbital and spin angular momenta $L = 1$ and $S = 1$, respectively, which couple via the SOC to form the total angular momentum $J = 0$. Considering the hybridization between neighbors, it is expected that the local singlets with $J = 0$ form a band to become a Van Vleck-type nonmagnetic insulator. In this context, Khaliullin has recently proposed a Van Vleck-type excitonic insulator, where an excitonic condensation between the local $J = 0$ and $J = 1$ states is driven by the magnetic order through the intersite exchange interaction [30].

The theoretical studies in the two extreme limits are important to investigate possible exotic states. However, it is highly desirable to examine the electronic ground state as well as the excitations in a wider range of couplings using a numerical technique which allows us to treat the interplay between the electron correlations and the SOC in a well controlled manner.

For this purpose, here we employ the multi-orbital dynamical mean field theory (DMFT) [31] to study a three-orbital Hubbard model with the SOC at four electrons per site, corresponding to the $(t_{2g})^4$ electronic configuration. We demonstrate that the interplay between the strong electron correlations and the SOC can stabilize the Van Vleck-type nonmagnetic insulator and its magnetic exciton condensation. Moreover, we find in the moderate electron correlation regime that the SOC can induce

a nonmagnetic excitonic insulator formed by an electron-hole pair in the $j = 1/2$ and $3/2$ based bands, as well as the relativistic band insulator. The characteristic features among these different insulators are found in the momentum resolved single-particle excitations.

The three-orbital Hubbard model with the relativistic SOC studied here is given as $H = H_0 + H_1$, where $H_0 = \sum_{\langle i,i' \rangle} \sum_{\gamma,\sigma} t^\gamma c_{i\gamma\sigma}^\dagger c_{i'\gamma\sigma} - \mu \sum_{i,\gamma,\sigma} n_{i\sigma}^\gamma + \lambda \sum_i \sum_{\gamma,\delta} \sum_{\sigma,\sigma'} \langle \gamma | \mathbf{l}_i | \delta \rangle \cdot \langle \sigma | \mathbf{s}_i | \sigma' \rangle c_{i\gamma\sigma}^\dagger c_{i\delta\sigma'}$ and $H_1 = U \sum_{i,\gamma} n_{i\gamma}^\uparrow n_{i\gamma}^\downarrow + \frac{U' - J_z}{2} \sum_{i,\gamma \neq \delta, \sigma} n_{i\sigma}^\gamma n_{i\sigma}^\delta + \frac{U'}{2} \sum_{i,\gamma \neq \delta, \sigma} n_{i\sigma}^\gamma n_{i\sigma}^\delta - J_{xy} \sum_{i,\gamma \neq \delta} c_{i\gamma\uparrow}^\dagger c_{i\gamma\downarrow} c_{i\delta\downarrow}^\dagger c_{i\delta\uparrow} + J_{xy} \sum_{i,\gamma \neq \delta} c_{i\gamma\uparrow}^\dagger c_{i\gamma\downarrow}^\dagger c_{i\delta\downarrow} c_{i\delta\uparrow}$. H_0 represents the non-interacting part, where t^γ sets the nearest-neighbor hopping amplitude for t_{2g} orbitals $\gamma = (d_{yz}, d_{zx}, d_{xy})$ and μ is the chemical potential tuned to be at four electrons per site. λ is the SOC and \mathbf{l}_i (\mathbf{s}_i) is the orbital (spin) angular momentum operator at site i . $c_{i\gamma\sigma}^\dagger$ is an electron creation operator at site i with orbital γ and spin $\sigma (= \uparrow, \downarrow)$ and $n_{i\sigma}^\gamma = c_{i\gamma\sigma}^\dagger c_{i\gamma\sigma}$. The local interacting part H_1 includes the intra (inter) orbital Coulomb interaction U (U'), the Hund's rule coupling J_z , and the spin flip and pair hopping J_{xy} , where we set $U = U' + 2J_z$ and $J_z = J_{xy} = 0.15U$ [32]. The electron correlations as well as ordered states are treated by the multi-orbital DMFT on the Bethe lattice with coordination number $Z \rightarrow \infty$ [33, 34], where the DMFT is exact. We consider the same bandwidth W for the three orbitals ($t^\gamma = t/\sqrt{Z}$), i.e., $W = 4t$, and t is used as the energy unit. In the following, we show the results for the lowest temperature $T = 0.06$, which essentially represent the ground state.

In the multi-orbital DMFT calculation, we numerically obtain the imaginary-time Green's functions in the impurity site $G_{\gamma,\sigma}^{\delta,\sigma'}(\tau) \equiv -\langle T_\tau c_{i\gamma\sigma}(\tau) c_{i\delta\sigma'}^\dagger(0) \rangle$ by using a continuous-time quantum Monte Carlo (CTQMC) method based on the strong coupling expansion [35]. Although the CTQMC calculation in principle enables us to solve the model exactly, the negative sign problem is one of the serious issues, particularly at low temperatures for large SOC. Our previous study for $(t_{2g})^5$ correlated systems have demonstrated that the sign problem is improved by transforming the t_{2g} orbital bases ($c_{i\gamma\sigma}$) to the maximally spin-orbit-entangled j bases (a_{ijm}) of the eigenstates of H_0 in the atomic limit, i.e.,

$$\begin{pmatrix} a_{i\frac{1}{2}\frac{3}{2}} \\ a_{i\frac{3}{2}\frac{3}{2}} \\ a_{i\frac{3}{2}\frac{-3}{2}} \end{pmatrix} = \frac{1}{\sqrt{6}} \begin{pmatrix} \sqrt{2} & -i\sqrt{2}s & \sqrt{2}s \\ s & -i & -2 \\ -\sqrt{3}s & -i\sqrt{3} & 0 \end{pmatrix} \begin{pmatrix} c_{id_{yz}\bar{\sigma}} \\ c_{id_{zx}\bar{\sigma}} \\ c_{id_{xy}\bar{\sigma}} \end{pmatrix},$$

where $s = 1$ (-1) for $\sigma = \uparrow$ (\downarrow) and $\bar{\sigma}$ implies the opposite spin to σ [19, 36]. We find that the same basis transformation can improve the sign problem also for the present $(t_{2g})^4$ systems.

We investigate two ordered states attributed to the interplay between the electron correlations and the

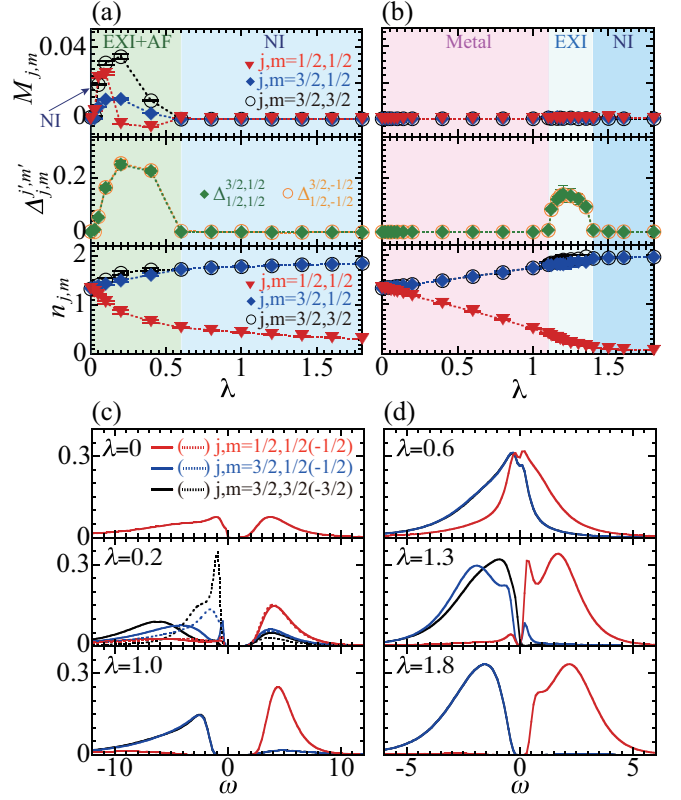


FIG. 1: (Color online) (a) and (b): λ dependence of staggered magnetization $M_{j,m}$ (top), excitonic order parameter $\Delta_{j,m}^{j',m'}$ (middle), and electron density $n_{j,m}$ (bottom). (c) and (d): Single-particle excitations spectrum $A_{j,m}(\omega)$ for three different λ 's. Note that, except for $\lambda = 0.2$ in (c), all components of the spectra are degenerate for $\lambda = 0$ in (c), $A_{j,m}(\omega) = A_{j,-m}(\omega)$ for $\lambda = 1.3$ in (d), and $A_{3/2,\pm 3/2}(\omega) = A_{3/2,\pm 1/2}(\omega)$ and $A_{j,m}(\omega) = A_{j,-m}(\omega)$ for other three parameters. We set $U = 12$ [(a) and (c)] and 3 [(b) and (d)]. EXI, EXI+AF, and NI stand for excitonic insulator, antiferromagnetic excitonic insulator, and nonmagnetic insulator, respectively.

SOC. The first state considered is the magnetic order along the z direction described by the order parameter $M_{j,m}(l) = \frac{1}{2} \sum_{m'=\pm m} \text{sign}(m') \langle a_{ljm}^\dagger a_{ljm'} \rangle$, where $l (= A, B)$ indicates two sublattices [37]. We also introduce the excitonic order parameter formed in different j orbitals, i.e., $\Delta_{j,m}^{j',m'}(l) = \langle a_{ljm}^\dagger a_{lj'm'} \rangle$, where $j \neq j'$. In addition, we calculate the electron density $n_{j,m}(l) = \sum_{m'=\pm m} \langle a_{ljm}^\dagger a_{ljm'} \rangle$. Since we have found that $M_{j,m}(A) = -M_{j,m}(B)$, implying AF order, $\Delta_{j,m}^{j',m'}(A) = -\Delta_{j,-m}^{j',-m'}(B)$, and $n_{j,m}(A) = n_{j,-m}(B)$, we omit the sublattice index l in these quantities below.

We first examine a case with large U . Figure 1(a) shows $M_{j,m}$, $\Delta_{j,m}^{j',m'}$, and $n_{j,m}$ for $U = 12$ as a function of λ . When $\lambda = 0$, there are no magnetic and excitonic orders with $n_{j,m} = 4/3$. However, as soon as λ is finite, the excitonic order parameters become finite with $\Delta_{j,m}^{3/2,1/2} = \Delta_{j,m}^{3/2,-1/2} \neq 0$. Concomitantly, the magnetic

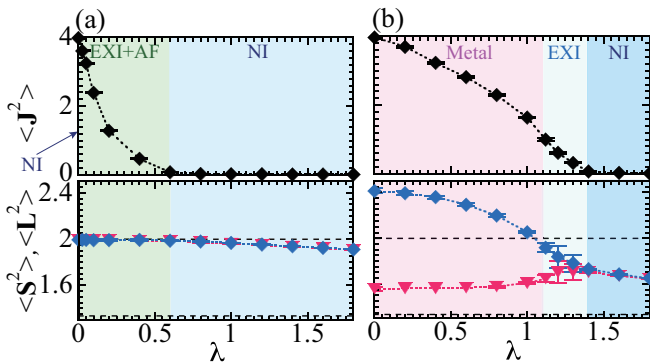


FIG. 2: (Color online) λ dependence of total angular momentum squared ($\langle \mathbf{J}^2 \rangle$) (top) and local spin (orbital) angular momentum squared ($\langle \mathbf{S}^2 \rangle$) ($\langle \mathbf{L}^2 \rangle$) (bottom) for (a) $U = 12$ and (b) $U = 3$. Dashed lines in bottom panels indicate $\langle \mathbf{S}^2 \rangle = \langle \mathbf{L}^2 \rangle = 2$ and $4/3$. EXI, EXI+AF, and NI stand for excitonic insulator, antiferromagnetic excitonic insulator, and nonmagnetic insulator, respectively.

order parameters are also finite for all three j components and are antiferromagnetically aligned. This phase extends up to $\lambda = 0.6$. It should also be noticed that $n_{3/2,1/2} \neq n_{3/2,3/2}$ in the presence of a finite excitonic order [38]. For $\lambda \geq 0.6$, both magnetic and excitonic orders disappear, and $n_{3/2,1/2} = n_{3/2,3/2}$ ($n_{1/2,1/2}$) increases (decreases) towards two (zero) with further increasing λ . In Fig. 1(c), we calculate the single-particle excitation spectrum $A_{j,m}(\omega) = -\frac{1}{\pi} \text{Im} G_{j,m}^{j,m}(\omega+i0)$, where $G_{j,m}^{j,m'}(\tau) \equiv -\langle T_\tau a_{ijm}(\tau) a_{ij'm'}^\dagger(0) \rangle$ and ω is real frequency, and find that there is a finite gap at the Fermi energy for all values of λ . Therefore, these states are all insulating.

To understand the nature of these insulating states, we examine the local spin and orbital angular momenta squared, $\langle \mathbf{S}_i^2 \rangle$ and $\langle \mathbf{L}_i^2 \rangle$, respectively, and the local total angular momentum squared ($\langle \mathbf{J}_i^2 \rangle$), where $\mathbf{S}_i = \sum_{\gamma} \sum_{\sigma,\sigma'} \langle \sigma | \mathbf{s}_i | \sigma' \rangle c_{i\gamma\sigma}^\dagger c_{i\gamma\sigma'}$, $\mathbf{L}_i = \sum_{\gamma,\delta} \sum_{\sigma} \langle \gamma | \mathbf{l}_i | \delta \rangle c_{i\gamma\sigma}^\dagger c_{i\delta\sigma}$, and $\mathbf{J}_i = \mathbf{S}_i - \mathbf{L}_i$. Since these quantities do not depend on the site index i , we simply omit this index hereafter. First, it is highly instructive to consider four limiting cases. According to the Hund's rule, when the electron correlation is significantly large with no SOC, we expect that $\langle \mathbf{S}^2 \rangle = \langle \mathbf{L}^2 \rangle = 2$ and $\langle \mathbf{J}^2 \rangle = 4$ because $\langle \mathbf{L} \cdot \mathbf{S} \rangle = 0$. If the SOC is introduced in this limit, the spin and orbital angular momenta are aligned antiparallel, and thus $\langle \mathbf{S}^2 \rangle = \langle \mathbf{L}^2 \rangle = 2$ and $\langle \mathbf{J}^2 \rangle = 0$. This is exactly the case for the ideal Van Vleck-type insulator. In the limit of significantly large SOC, where the ground state is expected to be the relativistic band insulator, $\langle \mathbf{S}^2 \rangle = \langle \mathbf{L}^2 \rangle = \frac{4}{3}$ and $\langle \mathbf{J}^2 \rangle = 0$. Finally, in the noninteracting limit without the SOC, $\langle \mathbf{S}^2 \rangle = 1.2$, $\langle \mathbf{L}^2 \rangle = 3.2$, and $\langle \mathbf{J}^2 \rangle = 4.4$.

Figure 2(a) shows the evolution of these quantities with varying λ for $U = 12$. As expected in the strong elec-

tron correlation limit, we find that $\langle \mathbf{S}^2 \rangle = \langle \mathbf{L}^2 \rangle = 2$ and $\langle \mathbf{J}^2 \rangle = 4$ for $\lambda = 0$, in accordance with the Hund's rule. With increasing λ , $\langle \mathbf{J}^2 \rangle$ monotonically decreases and eventually becomes zero for $\lambda \geq 0.6$, where neither magnetic nor excitonic order exists, as shown in Fig. 1(a). In this region, $\langle \mathbf{S}^2 \rangle$ and $\langle \mathbf{L}^2 \rangle$ are still close to two, specially near $\lambda = 0.6$, implying that the nonmagnetic insulator for $\lambda \geq 0.6$ is the Van Vleck-type insulator. However, we also notice that $\langle \mathbf{S}^2 \rangle$ and $\langle \mathbf{L}^2 \rangle$ gradually decreases with further increasing λ , while $\langle \mathbf{J}^2 \rangle$ is exactly zero, and we expect that $\langle \mathbf{S}^2 \rangle$ and $\langle \mathbf{L}^2 \rangle$ eventually become $4/3$ in the limit of $\lambda \rightarrow \infty$. Namely, the Van Vleck-type insulator is smoothly connected to the simple relativistic band insulator. On the other hand, we find in the region of $0 < \lambda < 0.6$ that $\langle \mathbf{J}^2 \rangle > 0$ while $\langle \mathbf{S}^2 \rangle$ and $\langle \mathbf{L}^2 \rangle$ remain two. In this region, the magnetic and excitonic orders are both finite, and therefore we attribute this phase to the magnetic excitonic insulator with the enhanced hybridization between the nonmagnetic $J = 0$ state and the magnetic $J \neq 0$ excited states.

Next, we examine a case with moderate $U = 3$. It is noticed first in Fig. 2(b) that $\langle \mathbf{J}^2 \rangle$, $\langle \mathbf{S}^2 \rangle$, and $\langle \mathbf{L}^2 \rangle$ for $\lambda = 0$ are clearly depart from the noninteracting values, implying that the electron correlations are indeed considered to be moderated, as it is expected for $U \approx W$. As shown in Fig. 1(b), we find no magnetic order for all values of λ . $A_{j,m}(\omega)$ exhibits sharp quasiparticle peaks around the Fermi energy for both $j = 1/2$ and $3/2$ when $\lambda < 1.2$ [see Fig. 1(d)], and thus the ground state for $\lambda < 1.2$ is metallic. However, the quasiparticle peaks disappear with further increasing λ and the metal-insulator transition occurs at $\lambda \sim 1.2$, where the single-particle excitation gap is open. More interestingly, in the intermediate SOC region for $1.2 \leq \lambda \leq 1.4$, we find that the excitonic insulator emerges without magnetic order [see Fig. 1(b)]. As shown in Fig. 1(d), the degeneracy of $A_{j=3/2,m}(\omega)$ for $m = \pm 1/2$ and $\pm 3/2$ is lifted in this phase. With further increasing λ , the excitonic order disappears for $\lambda > 1.4$ and the $j = 3/2$ based bands are almost completely occupied with a finite excitation gap to the unoccupied $j = 1/2$ based band [see Figs. 1(b) and 1(d)]. This implies that the ground state for $\lambda > 1.4$ is the relativistic band insulator. In the noninteracting limit, the SOC drives a transition from the metal to the relativistic band insulator at $\lambda = 4/3$. Therefore, the excitonic insulator found here is induced by the electron correlations just before the overlap between the $j = 1/2$ and $3/2$ based bands is diminished, where the condensation of an electron-hole pair in the $j = 1/2$ and $3/2$ based bands is most favorable with nonzero $\Delta_{1/2,\pm 1/2}^{3/2,\pm 1/2}$.

Let us now discuss the difference between the two excitonic insulators, i.e., the nonmagnetic excitonic insulator for moderate U and the magnetic excitonic insulator for large U . The former appears between the metal and the relativistic band insulator, where an electron-hole pair in

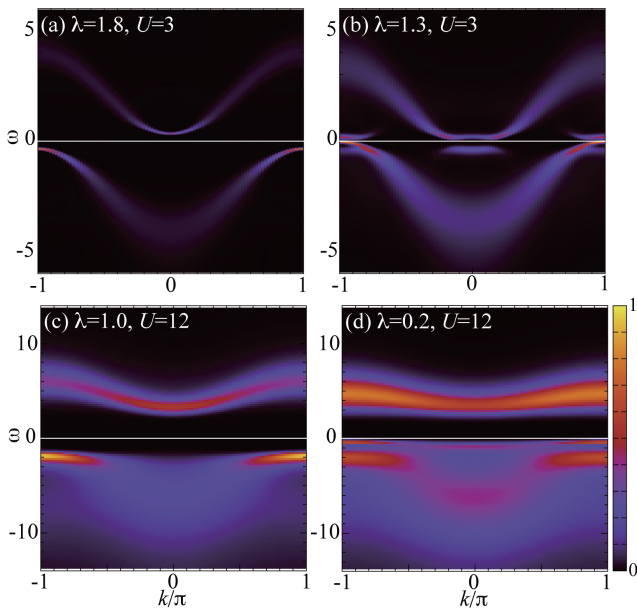


FIG. 3: (Color online) k -resolved single-particle spectral function $A(k, \omega)$ for relativistic band insulator, (b) nonmagnetic excitonic insulator, (c) Van Vleck-type nonmagnetic insulator, and (d) magnetic excitonic insulator. The maximum of each spectral function is normalized to be one. The Fermi energy is denoted by horizontal lines at $\omega = 0$.

the $j = 1/2$ and $3/2$ based bands are condensed. Therefore, the exciton condensation is similar to the conventional one where a valence hole and a conduction electron form a pair. In contrast, the other excitonic insulator appears in the strong coupling regime where U alone can open the single-particle excitation gap without magnetic order (see Fig. 1 for $\lambda = 0$). As shown in Fig. 2(a), in this strong coupling regime, the LS coupling scheme is a better description and thus the excitonic insulator here, accompanying the magnetic order, is considered as the Van Vleck-type excitonic insulator induced by mixing the nonmagnetic $J = 0$ state and the magnetic $J = 1$ and $J = 2$ excited states. This is simply because $\langle \mathbf{J}^2 \rangle > 2$ is possible only when the $J = 2$ state is involved. Indeed, we can readily show that the finite order parameter $\Delta_{1/2, \pm 1/2}^{3/2, \pm 1/2}$ generates the mixing between the $J = 0$ singlet and the $J = 2$ quintets in addition to the $J = 1$ triplets. Therefore, this magnetic excitonic insulator is similar to the one proposed by Khaliullin [30] except for the involvement of the $J = 2$ quintets.

Finally, we calculate the momentum resolved single-particle spectral function $A(k, \omega) = -\frac{1}{\pi} \sum_{jm} \text{Im} \mathcal{G}_{j,m}^{j,m}(k, \omega + i0)$ and examine the characteristic features in the single-particle excitations for the different insulating states found here. In our calculations, the single-particle Green's function $\mathcal{G}_{j,m}^{j,m}(k, \omega)$ is introduced within the cluster perturbation theory [39]. Since the DMFT includes the momentum k dependence only through the noninteracting energy dispersion $\epsilon(k)$, we introduce k to parametrize $\epsilon(k)$ as $\epsilon(k) = -2 \cos k$ [40].

The typical results of $A(k, \omega)$ are summarized in Fig. 3 for the four different insulators. As shown in Fig. 3(a), $A(k, \omega)$ for the relativistic band insulator in the moderate correlation regime is very similar to the noninteracting band structure for large λ and exhibits an indirect gap between the $j = 1/2$ and $3/2$ based bands. With slightly decreasing the SOC, the ground state becomes the nonmagnetic excitonic insulator and the typical result of $A(k, \omega)$ is shown in Fig. 3(b). This result clearly demonstrates the strong hybridization between the bottom of the $j = 1/2$ based conduction band and the top of the $j = 3/2$ based valence bands to induce a finite gap at the Fermi energy, and this is a strong evidence for the excitonic insulator [see also Fig. 1(d)]. It is also noticed in Fig. 3(b) that the spectrum is rather broad, as compared with the one for the relativistic band insulator shown in Fig. 3(a), despite that U is the same for both cases.

Figure 3 (c) represents the result for the Van Vleck-type insulator which appears in the strong correlation regime. The apparent difference from the moderate correlation regime is that the single-particle excitation gap is determined by U and the spectrum is rather featureless with a much broader structure specially in the unoccupied states. The typical result for the magnetic excitonic insulator is shown in Fig. 3(d). Similar to the Van Vleck-type insulator, $A(k, \omega)$ exhibits a broad structure. In addition, there exists a characteristic peak structure near $\omega = 0$ below the Fermi energy. The dispersion of this excitation is strongly renormalized to become almost flat, implying the strong correlation effects. As shown in Fig. 1(c), this excitation originates mainly from the one with the $m = \pm 1/2$ character of $j = 3/2$, the fourfold degeneracy of $j = 3/2$ being lifted due to the magnetic excitonic order.

In summary, we have studied the three-orbital Hubbard model with the SOC at four electrons per site by using the multi-orbital DMFT and the CTQMC method. For large U , we have demonstrated that the moderate SOC induces the Van Vleck-type nonmagnetic insulator, which is smoothly connected to the relativistic band insulator for larger λ . We have also found in the strong electron correlation regime that the magnetic excitonic insulator is induced for small λ by hybridizing the nonmagnetic $J = 0$ singlet of the local $(t_{2g})^4$ manifold and the excited multiplets such as $J = 1$ triplets and $J = 2$ quintets. More interestingly, we have found in the moderate electron correlation regime that the excitonic insulator emerges without any magnetic order. This excitonic insulator is due to the condensation of an electron-hole pair in the $j = 1/2$ and $3/2$ based bands. Although our results for moderate U are most appropriate for $5d$ transition metal oxides, the results for large U should also be relevant to $3d$ and $4d$ transition metal oxides with the low spin configuration. The different insulators found here are manifested most clearly in the momentum resolved

single-particle excitations, and thus can be observed in angle-resolved photoemission spectroscopy experiments.

The authors are grateful to K. Seki for valuable discussion. The numerical computations have been performed with facilities at Supercomputer Center in ISSP, Information Technology Center, University of Tokyo, and with the RIKEN supercomputer system (HOKUSAI Great-Wave). This work has been supported by Grant-in-Aid for Scientific Research from MEXT Japan under the Grant No. 25287096 and also in part by RIKEN iTHES Project and Molecular Systems.

-
- [1] J. J. Randall, L. Katz, and R. Ward, *J. Am. Chem. Soc.* **79**, 266 (1957).
- [2] R. J. Cava, B. Batlogg, K. Kiyono, H. Takagi, J. J. Krajewski, W. F. Peck, Jr., L. W. Rupp, Jr., and C. H. Chen, *Phys. Rev. B* **49**, 11890 (1994).
- [3] T. Shimura, Y. Inaguma, T. Nakamura, M. Itoh, and Y. Morii, *Phys. Rev. B* **52**, 9143 (1995).
- [4] G. Cao, J. Bolivar, S. McCall, J. E. Crow, and R. P. Guertin, *Phys. Rev. B* **57**, R11039 (1998).
- [5] H. Okabe, M. Isobe, E. Takayama-Muromachi, A. Koda, S. Takeshita, M. Hiraiishi, M. Miyazaki, R. Kadono, Y. Miyake, and J. Akimitsu, *Phys. Rev. B* **83**, 155118 (2011).
- [6] S. Sugano, Y. Tanabe, and H. Kamimura, *Multiplets of Transition-Metal Ions in Crystals* (Academic Press, New York, 1970).
- [7] B. J. Kim, Hosub Jin, S. J. Moon, J.-Y. Kim, B.-G. Park, C. S. Leem, Jaejun Yu, T. W. Noh, C. Kim, S.-J. Oh, J.-H. Park, V. Durairaj, G. Cao, and E. Rotenberg, *Phys. Rev. Lett.* **101**, 076402 (2008).
- [8] B. J. Kim, H. Ohsumi, T. Komesu, S. Sakai, T. Morita, H. Takagi, T. Arima, *Science* **323**, 1329 (2009).
- [9] K. Ishii, I. Jarrige, M. Yoshida, K. Ikeuchi, J. Mizuki, K. Ohashi, T. Takayama, J. Matsuno, and H. Takagi, *Phys. Rev. B* **83**, 115121 (2011).
- [10] S. Fujiyama, H. Ohsumi, T. Komesu, J. Matsuno, B. J. Kim, M. Takata, T. Arima, and H. Takagi, *Phys. Rev. Lett.* **108**, 247212 (2012).
- [11] G. Jackeli and G. Khaliullin, *Phys. Rev. Lett.* **102**, 017205 (2009).
- [12] H. Jin, H. Jeong, T. Ozaki, and J. Yu, *Phys. Rev. B* **80**, 075112 (2009).
- [13] H. Watanabe, T. Shirakawa, and S. Yunoki, *Phys. Rev. Lett.* **105**, 216410 (2010).
- [14] T. Shirakawa, H. Watanabe, and S. Yunoki, *J. Phys.: Conf. Ser.* **273**, 012148 (2011).
- [15] C. Martins, M. Aichhorn, L. Vaugier, and S. Biermann, *Phys. Rev. Lett.* **107**, 266404 (2011).
- [16] R. Arita, J. Kuneš, A. V. Kozhevnikov, A. G. Eguiluz, and M. Imada, *Phys. Rev. Lett.* **108**, 086403 (2012).
- [17] H. Onishi, *J. Phys.: Conf. Ser.* **391**, 012102 (2012).
- [18] H. Watanabe, T. Shirakawa, and S. Yunoki, *Phys. Rev. B* **89**, 165115 (2014).
- [19] T. Sato, T. Shirakawa, and S. Yunoki, *Phys. Rev. B* **91**, 125122 (2015).
- [20] F. Wang and T. Senthil, *Phys. Rev. Lett.* **106**, 136402 (2011).
- [21] H. Watanabe, T. Shirakawa, and S. Yunoki, *Phys. Rev. Lett.* **110**, 027002 (2013).
- [22] Y. Yang, W.-S. Wang, J.-G. Liu, H. Chen, J.-H. Dai, and Q.-H. Wang, *Phys. Rev. B* **89**, 094518 (2014).
- [23] Z. Y. Meng, Y. B. Kim, and H.-Y. Kee, *Phys. Rev. Lett.* **113**, 177003 (2014).
- [24] Y. Shi, Y. Guo, Y. Shirako, W. Yi, X. Wang, A. A. Belik, Y. Matsushita, H. L. Feng, Y. Tsujimoto, M. Arai, N. Wang, M. Akaogi, and K. Yamaura, *J. Am. Chem. Soc.* **135**, 16507-16516 (2013).
- [25] P. Zheng, Y. G. Shi, A. F. Fang, T. Dong, K. Yamaura, and N. L. Wang, *J. Phys.: Condens. Matter* **26**, 435601 (2014).
- [26] M. Bremholm, S. E. Dutton, P. W. Stephens, and R. J. Cava, *J. Solid State Chem.* **184**, 601 (2011).
- [27] L. Du, X. Sheng, H. Weng, and X. Dai, *Europhys. Lett.* **101**, 27003 (2013).
- [28] M.-C. Jung and K.-W. Lee, *Phys. Rev. B* **90**, 045120 (2014).
- [29] L. Du, L. Huang, and X. Dai, *Eur. Phys. J. B* **86**, 94 (2013).
- [30] G. Khaliullin, *Phys. Rev. Lett.* **111**, 197201 (2013).
- [31] L. Kotliar, S. Y. Savrasov, G. Pálsson, and G. Biroli, *Phys. Rev. Lett.* **87**, 186401 (2001).
- [32] J. Kanamori, *Prog. Theor. Phys.* **30**, 275 (1963).
- [33] W. Metzner and D. Vollhardt, *Phys. Rev. Lett.* **62**, 324 (1989).
- [34] M. Eckstein, M. Kollar, K. Byczuk, and D. Vollhardt, *Phys. Rev. B* **71**, 235119 (2005).
- [35] P. Werner, A. Comanac, L. de Medici, M. Troyer, and A. J. Millis, *Phys. Rev. Lett.* **97**, 076405 (2006).
- [36] The imaginary unit i in the transformation matrix should not be confused with the site index i in the annihilation operators.
- [37] Since our model is isotropic, the magnetic orders along the other x and y directions are identical to that along the z direction.
- [38] This is also the case in another excitonic insulating phase for $U = 3$.
- [39] D. Sénéchal, D. Perez, and M. Pioro-Ladrière, *Phys. Rev. Lett.* **84**, 522 (2000).
- [40] S. Hoshino, J. Otsuki, and Y. Kuramoto, *J. Phys. Soc. Jpn.* **82**, 044707 (2013).